

The MaxFlux algorithm for calculating variationally optimized reaction paths for conformational transitions in many body systems at finite temperature

Shuanghong Huo and John E. Straub^{a)}

Department of Chemistry, Boston University, Boston, Massachusetts 02215

(Received 29 April 1997; accepted 26 June 1997)

An algorithm for the calculation of reaction paths between known reactant and product states in systems of low or high dimension is described. The optimal reaction path is defined as the path of maximum flux for a diffusive dynamics assuming isotropic friction. The resulting reaction path is temperature dependent and independent of the magnitude of the friction. Comparison is made with a number of algorithms designed for the calculation of minimum-energy reaction paths. Applications to two model potentials and an extended atom model of a dipeptide are presented. The applications demonstrate the ability of the algorithm to isolate a temperature-dependent optimal reaction path for a high dimensional molecular system. © 1997 American Institute of Physics. [S0021-9606(97)01437-2]

I. INTRODUCTION

In estimating the reaction rate for a chemical reaction the careful identification of a “good” reaction coordinate is crucial. The mechanism of the reaction depends entirely on this choice. For activated processes, the absolute reaction rate constant is very sensitive to the choice of the reaction coordinate which determines the activation energy and the magnitude of dynamical corrections entering through the transmission coefficient. The choice is further complicated by the fact that the reaction coordinate and the reaction mechanism can depend on the temperature.

The best reaction path must be chosen from an infinite number of possible paths connecting the initial and final structures. Its identification can prove to be a difficult problem in isolated and relatively small molecular reaction systems. Methods based on a directed search of the potential surface coupled with local energy minimization work well on few-dimensional systems.¹ Methods based on a knowledge of initial and final states and a subsequent refinement of the path by a line search have been proposed and found some success.²⁻⁵

An important innovation was made independently by Elber and Karplus⁶ and by Pratt.⁷ They proposed to generate a trial path connecting known initial (reactant) and final (product) configurations. The trial path is subsequently refined based on the extremization of a functional defining the optimal path. In the method of Elber and co-workers,⁸⁻¹⁰ the intermediate configurations defining the trial path are simultaneously optimized to minimize the objective function⁸

$$\mathcal{S} = \frac{1}{L} \int_{\mathbf{r}_R}^{\mathbf{r}_P} U(\mathbf{r}) d\mathbf{l}(\mathbf{r}). \quad (1)$$

$\mathbf{l}(\mathbf{r})$ is the reaction path (a line) connecting the known initial (\mathbf{r}_R) and final (\mathbf{r}_P) structures, $U(\mathbf{r})$ is the potential energy of the system for a given configuration \mathbf{r} and $L = \int d\mathbf{l}(\mathbf{r})$ is the

path length. It has been demonstrated that this algorithm provides a good estimate of the zero-temperature reaction path between known initial and final structures for reactions ranging from the chair-boat isomerization of cyclohexane,⁸ to conformational changes in a tetrapeptide,⁹ to ligand diffusion in myoglobin.⁸ Related methods based on a modified criterion for the optimal path have also been developed.¹¹

A shortcoming of this method is that the path which minimizes \mathcal{S} may not be the path with the maximum rate of transition between reactants and products. Another shortcoming is that the definition of the optimal reaction path is independent of the temperature.

Elber^{12,13} has recently proposed an elegant method for the evaluation of a reaction path at nonzero temperature. The method defines the optimal reaction pathway as one which maximizes the conditional probability for moving between \mathbf{r}_R to \mathbf{r}_P in time t by a Langevin dynamics proposed by Onsager and Machlup.¹⁴ A functional integral is evaluated out over all paths for the set $\mathbf{R} = (\mathbf{r}_R, \mathbf{r}_1 \cdots \mathbf{r}_{M-1}, \mathbf{r}_P)$ of $M-1$ intermediate configurations \mathbf{r}_k connecting the reactant ($\mathbf{r}_0 = \mathbf{r}_R$) and product ($\mathbf{r}_M = \mathbf{r}_P$) configurations. The overall time for the transition from \mathbf{r}_R to \mathbf{r}_P is fixed at $t = M\Delta t$. A variation on this method has been used by Olender and Elber to integrate classical dynamical equations of motion using very large time steps with impressive results.¹⁵

Pathways with large conditional probabilities are expected to correspond to good reaction paths. The pathway that maximizes the conditional probability can be considered to be the optimal reaction path. Pratt presented a related method which similarly defines a reaction path using a chain of intermediate configurations connecting the reactant and product states.⁷ He proposed a conditional probability based on a Smoluchowski dynamics which is the high friction limit of the Langevin equation. In that sense, the method of Pratt appears to be equivalent to the more general method of Elber in the high friction limit where inertial motion can be ignored.

Gillian and Wilson¹⁶ presented a variational method for

^{a)} Author to whom correspondence should be addressed.

computing classical reaction paths with fixed initial (\mathbf{r}_R) and final (\mathbf{r}_P) positions. They found that their “discrete time” dynamics which defined a weight for moving between two points over a time increment Δt took the form of the position Verlet algorithm. In the low friction limit when the dynamics along the reaction path is dominated by inertial motion the conditional probability in Elber’s Onsager–Machlup action method is simply the Verlet integrator as found in the Gillian and Wilson study. Therefore, Elber’s Onsager–Machlup action method provides a variational method that encompasses inertial Hamiltonian flow and diffusive Smoluchowski dynamics.

An apparent improvement over the zero-temperature methods discussed above, in Elber’s Onsager–Machlup action method the temperature explicitly appears in the definition of the conditional probability for moving from reactant to product. However, the temperature only appears in a product with the “friction” γ . With some effort it is possible to compute the positional dependent friction coefficient for simple systems.¹⁷ However, in most applications we can expect to employ a fictional friction. This leaves the temperature, which only appears in ratios involving the friction, ill-defined.

Moreover, it is desirable to isolate the reaction pathway that corresponds to the maximum reaction rate of transition from reactant to product. In Elber’s Onsager–Machlup action method, the total time for the trajectory is given as input and is not optimized as a function of the path. Therefore, to identify a path of maximum rate of transition between reactants and products at a well-defined temperature, we appeal to variational rate theory.

In this paper, we present the “MaxFlux” algorithm for computing the reaction pathway of maximum diffusive flux. While the method is based on an overdamped diffusional dynamics, the definition of the optimal reaction pathway is found to be a function of a precisely defined temperature independent of any knowledge of the friction. Applications to model systems and a dipeptide demonstrate the ability of the method to isolate optimized reaction pathways in high dimensional molecular systems at nonzero temperature.

II. THE MAXFLUX METHOD

There is a long history of defining the optimal reaction pathway as one that maximizes the reaction rate or minimizes the mean first passage time between reactant and product states. This idea underlies variational transition state theory¹⁸ where the optimal transition state dividing surface is found to minimize the transition state theory rate estimate of the reaction rate constant.

For our purposes we focus on an overdamped diffusive dynamics where the probability distribution $p(\mathbf{r}, t)$ is well-described by the Smoluchowski equation¹⁹

$$\frac{\partial p(\mathbf{r}, t)}{\partial t} = -\nabla \cdot \mathbf{j} \quad (2)$$

with the flux

$$\mathbf{j}(\mathbf{r}, t) = -e^{-\beta U(\mathbf{r})} \mathbf{D}(\mathbf{r}) \cdot \nabla [p(\mathbf{r}, t) e^{\beta U(\mathbf{r})}], \quad (3)$$

where the inertial effects are ignored. We restrict our discussion to a system with isotropic and spatially independent friction γ so that the diffusion tensor $\mathbf{D}(\mathbf{r}) = (k_B T / m \gamma) \mathbf{I}$, where \mathbf{I} is the identity matrix.

For a particle moving in a one-dimensional bistable potential along coordinate x , under stationary conditions [$\mathbf{j}(x, t) = \mathbf{j}(x)$], the flux $\mathbf{j}(x) = \text{constant}$, and the approximate forward reacting mean first passage time is¹⁹

$$\mathcal{T}(x_R \rightarrow x_P) = \frac{\gamma}{\omega_0} (2\pi m \beta)^{1/2} e^{-\beta U(x_R)} \int_{x_R}^{x_P} e^{\beta U(x)} dl(x). \quad (4)$$

This expression assumes that the barrier separating the wells is large compared to the thermal energy and that the reactant basin is well approximated as harmonic with a frequency ω_0 . When the remaining integral is approximated as $[2\pi / (m \beta \omega_B^2)]^{1/2} \exp[\beta U(x_B)]$, where x_B is the position of the barrier and ω_B is the barrier frequency, the result is the high friction Smoluchowski mean first passage time²⁰

$$\mathcal{T}(x_R \rightarrow x_P) = \frac{2\pi\gamma}{\omega_B \omega_0} e^{\beta[U(x_B) - U(x_R)]}. \quad (5)$$

The situation is more complicated in many dimensions. It has been demonstrated that for a narrow saddle, isotropic friction and high reduced barrier, it is reasonable to assume a constant flux along the path as the first passage time will be dominated by the flux in the saddle region.²¹ However, even under stationary conditions, one can not assume that $\mathbf{j}(\mathbf{r}) = \text{constant}$. Nevertheless, Berkowitz *et al.* assumed a constant flux along the reaction path, equivalent to assuming that all reactive trajectories are nonintersecting.^{21,22} They defined the optimal reaction path as the path $l(\mathbf{r})$ of “minimum resistance” where the resistance is proportional to the line integral²³

$$\mathcal{P} = \int_{\mathbf{r}_R}^{\mathbf{r}_P} e^{\beta U(\mathbf{r})} dl(\mathbf{r}) \quad (6)$$

for the case of an isotropic, spatially independent friction.²⁴

This approximate result agrees with the more exact result in one-dimension derived from the minimization of the mean first passage time. The result is also intuitively obvious in the case of high barriers where the line integral will be dominated by contributions in the barrier region and minimization of the integral is equivalent to isolating the path with the lowest activation barrier. However, there are two assumptions underlying the proposal that the path that minimizes Eq. (6) is the optimal reaction path. (1) Under the stationary reaction condition, the magnitude of flux along the trajectory which connects reactant and product configurations is constant. (2) The optimal path is dominant. It is reasonable to ignore the contribution to the reactive flux from paths that deviate from the optimal path.

The MaxFlux method developed in this paper rests on the minimum resistance principle and its assumptions.²³ It is

based on the identification of an optimal reaction path through the minimization of Eq. (6) by variationally optimizing the reaction path connecting \mathbf{r}_R and \mathbf{r}_P .

The discretized integral

$$\mathcal{A}(\mathbf{R}) = \sum_{k=0}^{M-1} e^{\beta U(\mathbf{r}_k)} |\mathbf{r}_{k+1} - \mathbf{r}_k| \quad (7)$$

can be thought of as a chain composed of $M+1$ copies of the N particle system at a series of positions $\mathbf{R} = (\mathbf{r}_R, \mathbf{r}_1 \dots \mathbf{r}_{M-1}, \mathbf{r}_P)$. Therefore, the chain is a set of instantaneous configurations along the path connecting the initial and final structures. Minimizing the line integral \mathcal{P} in Eq. (6) is equivalent to adjusting the positions of the monomers in the chain as long as the distances between successive monomers in the chain [the $dI(\mathbf{r})$ increments] are identical.

Following the ‘‘path’’ protocol of Elber and co-workers⁸ we minimize a discretized form of the line integral Eq. (7) with added restraints. (1) One restraint acts as a bond between nearest neighbor intermediate structures to encourage the mean-square distances between adjacent structures to be approximately constant

$$\mathcal{E}_A(\mathbf{R}) = \kappa \sum_{k=1}^M [(\mathbf{r}_k - \mathbf{r}_{k-1})^2 - d_{\text{ave}}^2]^2, \quad (8)$$

where $d_{\text{ave}}^2 = \sum_{k=1}^M (\mathbf{r}_k - \mathbf{r}_{k-1})^2 / M$. (2) A repulsive interaction between intermediates along the path⁸

$$\mathcal{E}_R(\mathbf{R}) = \frac{\rho}{\lambda} \sum_{j>k+1} \exp[-\lambda(\mathbf{r}_j - \mathbf{r}_k)^2 / \langle d \rangle^2] \quad (9)$$

is added where $\langle d \rangle = \sum_{k=1}^M (\mathbf{r}_k - \mathbf{r}_{k-1}) / M$ prevents two intermediates from coming too close to one another. This makes the path a self-avoiding walk. (3) For molecular systems there are constraints that eliminate rigid body translations and rotations⁸

$$\sum_{\mu=1}^N m_{\mu} (\mathbf{r}_{\mu} - \mathbf{r}_{\mu}^{\text{fix}}) = 0, \quad (10)$$

$$\sum_{\mu=1}^N m_{\mu} \mathbf{r}_{\mu} \times \mathbf{r}_{\mu}^{\text{fix}} = 0, \quad (11)$$

where N is the number of atoms in the system, m_{μ} is the atomic mass, and \mathbf{r}_{μ} the Cartesian coordinates for the μ th atom. $\{\mathbf{r}_{\mu}^{\text{fix}}\}_{\mu=1,N}$ is the arithmetic average of the coordinates of the atoms in the reactant and product configurations. These constraints are not needed for problems involving space-fixed potentials.

III. COMPUTATIONAL PROTOCOL

With the objective function defined as $\mathcal{O}(\mathbf{R}) = \mathcal{A}(\mathbf{R}) + \text{constraints}$, the problem is to find its global minimum value in the space of all possible reaction paths. In a large molecule such as a protein, this is a computationally demanding task. In our applications, we optimize the cost function using a simulated annealing protocol. We define the effective energy function

$$\mathcal{H} = \sum_{k=1}^{M-1} \left[\frac{1}{2} \sum_{\mu=1}^N m_{\mu} \dot{\mathbf{r}}_{k\mu}^2 + \mathcal{O}(\mathbf{R}) \right] \quad (12)$$

for the chain $\mathbf{R} = (\mathbf{r}_R, \mathbf{r}_1 \dots \mathbf{r}_{M-1}, \mathbf{r}_P)$ of intermediate configurations $\mathbf{r}_k = (\mathbf{r}_{1k}, \dots, \mathbf{r}_{\mu k}, \dots, \mathbf{r}_{Nk})$ each with N particles of mass m_{μ} . The reactant (\mathbf{r}_R) and product (\mathbf{r}_P) configurations are fixed. The annealing temperature in d dimensional space is defined by the average kinetic energy of the intermediate configurations

$$T_a = \frac{1}{dN(M-1)k_B} \sum_{k=1}^{M-1} \sum_{\mu=1}^N m_{\mu} \dot{\mathbf{r}}_{k\mu}^2. \quad (13)$$

There are two temperatures—the fictitious annealing temperature T_a and the actual temperature of the reaction system appearing as $1/\beta$ in Eq. (6). By minimizing \mathcal{H} at $T_a = 0$ we minimize $\mathcal{O}(\mathbf{R})$. When the constraints represent a small contribution to $\mathcal{O}(\mathbf{R})$ the pathway also represents a minimum of $\mathcal{A}(\mathbf{R})$ and a maximum of the integrated flux at nonzero temperature $1/\beta$.

Initially T_a is increased to a value on the order of the largest barriers in the configuration space of $\mathcal{O}(\mathbf{R})$ which is exponentially more rugged than $U(\mathbf{r})$. Rather than explicitly controlling T_a during the run, a damping term is added to the equation of motion for the μ th atom in the k th intermediate structure

$$m \ddot{\mathbf{r}}_{\mu k} = -\nabla_{\mathbf{r}_{\mu k}} \mathcal{O}(\mathbf{R}) - \zeta \dot{\mathbf{r}}_{\mu k}. \quad (14)$$

This equation of motion can be integrated using a finite difference algorithm proposed by Amara and Straub²⁵ to allow the chain of intermediates to sample a variety of possible reaction paths. The system dynamics allows the annealing temperature to fluctuate during the run. In the event that there is a phase change with an associated latent heat, the heat is added to the system to allow for larger fluctuations and additional sampling. The rate of temperature decrease is roughly proportional to ζ . Eventually the annealing temperature approaches zero and the chain will settle to an estimate of the reaction pathway of maximum flux.

IV. APPLICATIONS

We have applied the algorithm described above to two model potentials and a dipeptide. The results are described below.

A. Müller potential

The procedure defined above was followed in the first application to the two parameter model potential of Fukui, Kato and Fujimoto²⁶ studied by Müller,²

$$U_M(x, y) = -200e^{-(x-1)^2 - 10y^2} - 100e^{-x^2 - 10(y-0.5)^2} \\ - 170e^{-6.5(x+0.5)^2 + 11(x+0.5)(y-1.5) - 6.5(y-1.5)^2} \\ + 15e^{0.7(x+1)^2 + 0.6(x+1)(y-1) + 0.7(y-1)^2}. \quad (15)$$

This potential provides a good test of a ‘‘local’’ reaction path method which relies on a good initial guess at the path and subsequent refinement or a directed search in a few-

TABLE I. Parameters for the restraints and the annealing dynamics that were used in each optimization run.

	β	$M+1$	$\kappa(\times 10^{-4})$	$\rho(\times 10^{-2})$	λ	$T_d(\times 10^{-3})$	ζ	
Müller	0.06	7	5	30	2.0			
		12	5	16	2.0			
		25	5	7.35	2.0			
Three Hole	1.0	15	0.01	0.7	2.0			
		2.0	15	0.55	8.26	2.0		
		3.3	15	5	200	2.0	6.4	0.1
Dipeptide	1.678	15	5	200	2.0	15	0.1	
		7	0.5	30	2.0			

dimensional configuration space. The parameters for the optimization run are given in Table I. After setting λ in Eq. (9), the value of ρ is set such that the upper limit for the intermediate repulsion constraints \mathcal{E}_R is approximately 1% of the magnitude of the integrated flux \mathcal{P} for the initial guess. This “rule of thumb” was followed in all our applications.

The reaction pathway found by the MaxFlux algorithm is displayed in Fig. 1. The global path follows the optimal reaction pathway for the potential. A coarse chain ($M+1=7$) results in a jagged path which can be refined by increasing M and applying a simple energy minimization refinement rather than the simulated annealing procedure. In Fig. 1 the chain is further refined using $M+1=12, 25, 50$ which provides a smooth reaction path comparable to what would be defined by a minimum-energy path method. The MaxFlux computed reaction pathway is an estimate of the best path for the reaction system at nonzero temperature $1/\beta$.

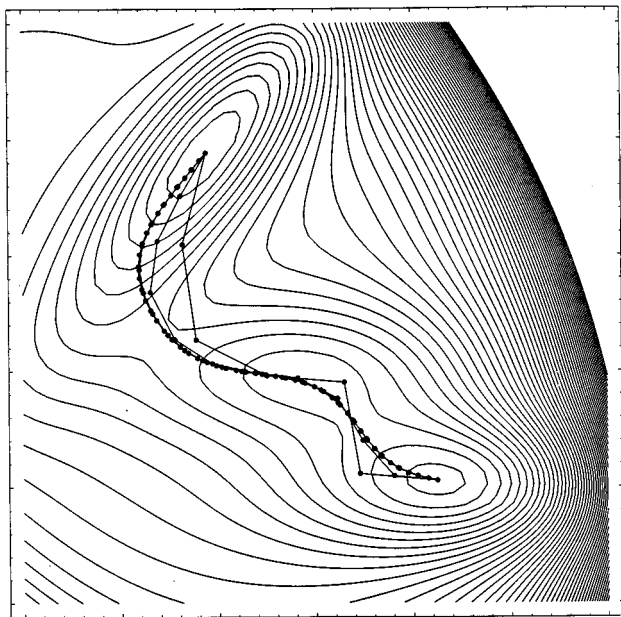


FIG. 1. The reaction path found for the Müller potential using $M+1=7, 12, 25,$ and 50 . The MaxFlux method is effective not only in isolating a globally optimized path but in providing a locally smooth reaction coordinate.

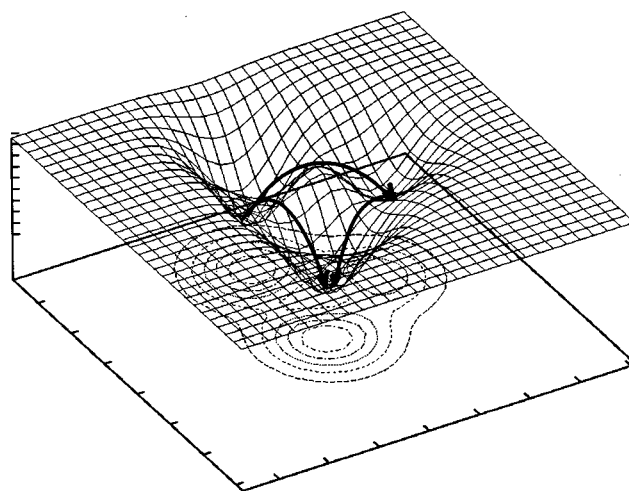


FIG. 2. A contour/surface plot of the three hole potential showing the three minima and saddles and the upper and lower reaction pathways. The arrows indicate the “upper” and “lower” reaction pathways.

B. Three hole potential

The Müller potential provides a good test for a minimum-energy refinement method but is not a challenging test of algorithms designed to isolate the globally optimal reaction path. For that purpose we examine a simple two-dimensional model potential,

$$U_{TH}(x,y) = -3.0e^{-x^2}[e^{-(y-5/3)^2} - e^{-(y-1/3)^2}] - 5.0e^{-y^2}[e^{-(x-1)^2} + e^{-(x+1)^2}] \quad (16)$$

which is shown in Fig. 2. In addition to the reactant (lower left well) and product (lower right well) minima there is a third energy minimum (above center). There are two possible reaction pathways. The lower reaction path moves roughly left-to-right between the reactant and product wells crossing a single saddle point. The upper reaction path travels indirectly over a lower saddle point, through a basin, and then down over a second saddle point before reaching the product state.

The best minimum-energy “zero-temperature” reaction path based on the minimization of Eq. (1) is the lower reaction path. However, the lower path is not always the path of maximum reaction rate at nonzero temperature. Assuming a diffusive dynamics and using Eq. (6) to define the reaction path of maximum flux, the lower reaction path will be the pathway of maximum flux only at high temperatures. At low enough temperatures the upper pathway, which crosses two lower energy saddle points, is dominant.

We have applied the MaxFlux algorithm to this potential at three temperatures which span the transition between the two reaction pathways (see Table I). The results are shown in Fig. 3. The optimized pathways follow the direct lower pathway at high temperatures. As the temperature is lowered there is a transition to the dominant upper pathway.

The integrand of Eq. (6) is shown in Fig. 4 as a function of the length of the reaction path. The initial guess is shown

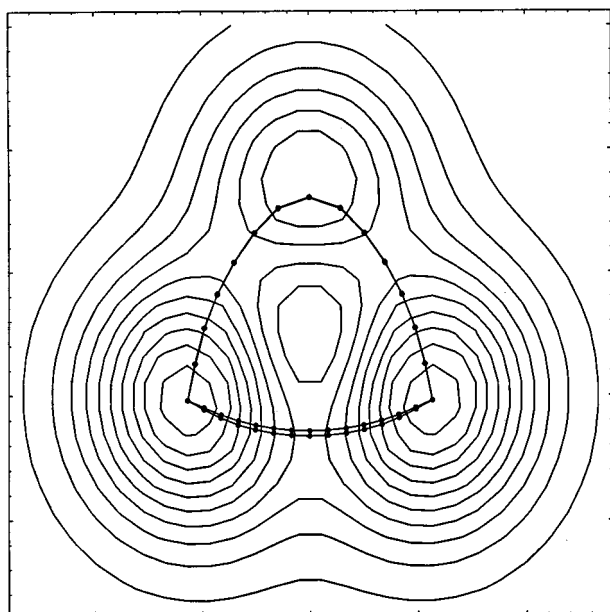


FIG. 3. The reaction path found for the three hole potential for three different values of the reaction system temperature (from top to bottom $\beta=3.3$, 1, and 2). The MaxFlux method is effective in isolating the dominant reaction pathway at high and low temperatures. Zero-temperature methods will define a single reaction coordinate which, in some temperature regime, will provide both an underestimate of the rate and the wrong reaction mechanism.

along with the optimized results for the upper and lower pathways at each temperature. At the temperature shown the upper reaction path provides the dominant reactive flux.

In Fig. 5 the contributions to the effective energy objec-

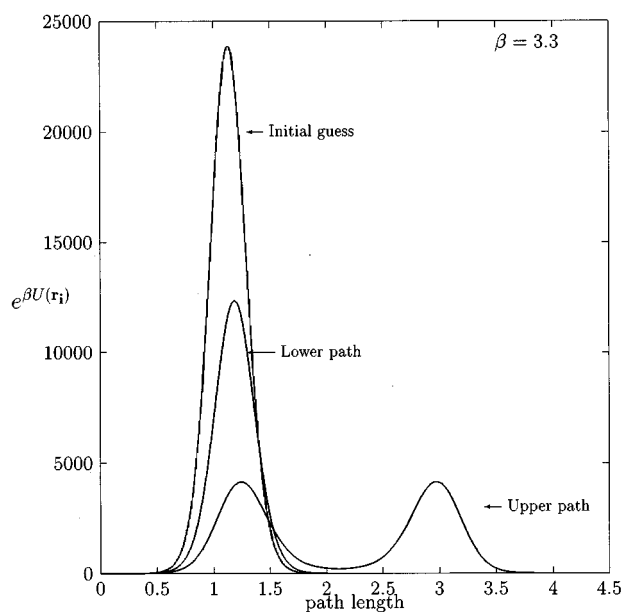


FIG. 4. The integrand $\exp[\beta U(\mathbf{r})]$ of Eq. (6) is shown for the upper and lower reaction pathways on the three hole potential for $\beta=3.3$. The integrated flux \mathcal{P} is 9698, 5506, and 4867 for the linear, lower path, and upper path, respectively (in reduced units). At this temperature, the upper reaction path provides the dominant reactive flux. The dominant reaction path is correctly identified by the MaxFlux method.

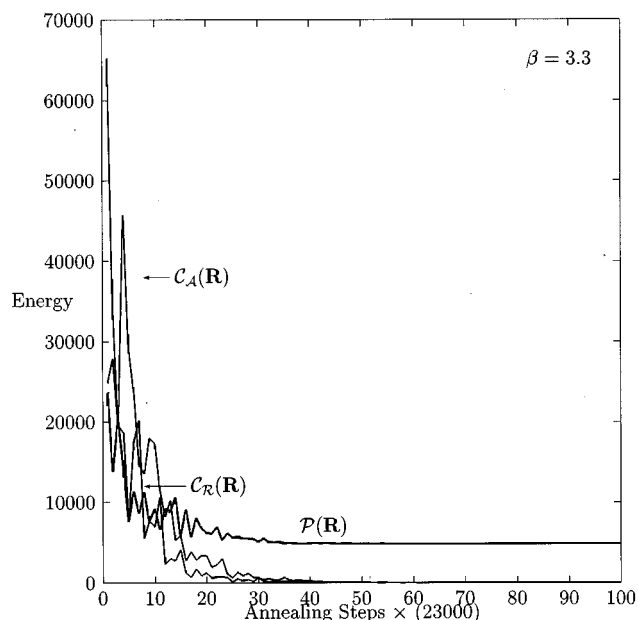


FIG. 5. The contributions to the objective function \mathcal{P} +constraints as a function of the number of annealing steps taken during the annealing run for $\beta=3.3$. The results are qualitatively the same at all temperatures studied. The individual contributions to the objective function including the integrated flux \mathcal{P} , the equal distance restraint \mathcal{C}_A , and intermediate repulsion \mathcal{C}_R are separately displayed. Asymptotically, the constraints are insignificant and the minimization of the objective function is equivalent to the minimization of \mathcal{P} alone.

tive function Eq. (6) are displayed as a function of the number of steps executed during the annealing run. While the annealing temperature, T_a , is zero at the run's end, the temperature of the reaction system, $1/\beta$, is fixed throughout the run. In each case, after initially large fluctuations in the energy the objective function relaxes to an optimal value. The constraint terms which can be large in the initial stages decay rapidly; at the end of the annealing run the constraints make a negligible contribution to the objective function.

For comparison we have applied the criterion of Elber⁸ in the form of Eq. (1) and the conjugate peak refinement method of Fischer and Karplus⁴ to the three hole potential. The Elber and Karplus definition of the best reaction path may be combined with a global optimization method to refine the path and minimize Eq. (1). We employed the same constraints used in applying the MaxFlux method. The Fischer and Karplus method does not lend itself to a global optimization protocol. The result is determined by the choice of initial path. The set of all possible initial paths may map onto one or more final reaction pathways. Both methods are minimum-energy reaction path methods; there is no dependence of the reaction path on the temperature.

In each case, we began with a straight line path as the initial guess. Using both the Elber and Karplus definition and the Fischer and Karplus method the lower reaction path was found to be optimal. At high enough temperatures, that is the dominant path. When the temperature is lowered the upper path is dominant. As a result the rate constant determined over the incorrect lower path will significantly underestimate the reaction rate.

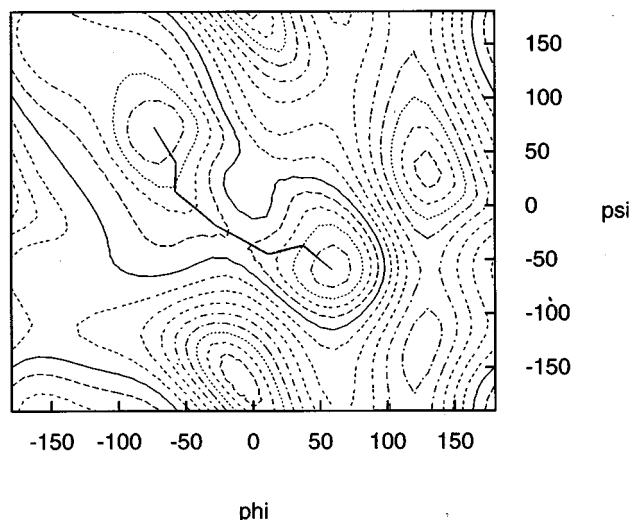


FIG. 6. The reaction path of dialanine on the adiabatic (ϕ , ψ) potential energy map. While the MaxFlux method is applied in Cartesian coordinate space the resulting reaction path is smooth as a function of the more natural ϕ and ψ angles.

C. Alanine dipeptide

The MaxFlux method was applied to an extended atom model of the alanine dipeptide studied previously by Czerminski and Elber.^{9,12} The CHARMM force field was used with the version 19 parameter set²⁷ with slightly altered charges and with the 1–4 electrostatic interaction scaling parameter set to 1.0.⁹ As in the previous study, a distance dependent dielectric constant is employed to model the solvent screening. There was no cutoff of the nonbonded interactions.

The potential energy of the reactant and product configurations is -7.63 and -8.30 kcal/mol, respectively. The initial guess was a straight line interpolation between reactant and product configurations defined in Cartesian coordinates. To relieve the bad contacts that result from the linear interpolation, a bit of constrained energy minimization was performed with the ϕ and ψ dihedral angles fixed. After the minimization, the highest energy of the intermediate configuration was -0.38 kcal/mol. In order to avoid numerical overflow problems, we minimized the modified objective function

$$\sum_{k=0}^{M-1} e^{\beta \Delta U(r)} |\mathbf{r}_{k+1} - \mathbf{r}_k| + \text{constraints}, \quad (17)$$

where $\Delta U(\mathbf{r}) = U(\mathbf{r}) - U_{\text{ref}}$. We chose the reference potential energy to be $U_{\text{ref}} = U(\mathbf{r}_R)$. The gradient projection technique⁹ was applied to ensure no rigid body translational or rotational motion.

Figure 6 shows the result of the MaxFlux algorithm for a temperature of 300 K projected onto the adiabatic (ϕ , ψ) energy map. At this temperature, the barrier separating the reactant and product state wells is large compared to the thermal energy. For this simple system the MaxFlux algorithm identifies a reaction pathway similar to that found by zero-

temperature reaction path methods. This test case serves to demonstrate the ease of application of the method to all atom models of biomolecular systems.

V. CONCLUSIONS

The determination of the optimal reaction pathway in a multidimensional system at finite (nonzero) temperature is a central problem in reaction rate theory. While a number of zero-temperature methods have been successful in estimating minimum energy reaction pathways in multidimensional systems, these pathways may grossly underestimate the actual reaction rate at finite temperature. The MaxFlux algorithm can be used to compute the reaction pathway of maximum reactive flux at a well-defined temperature in both low and high dimensional systems.

ACKNOWLEDGMENTS

J.E.S. gratefully acknowledges the Alfred P. Sloan Foundation and the Petroleum Research Fund of the American Chemical Society (30601-AC6) for support, and the National Science Foundation for support (CHE-9632236) and computational resources at the National Center for Supercomputing Applications (CHE-960010N). We thank A. M. Berezhkovskii for helpful comments.

- ¹C. J. Cerjan and W. H. Miller, *J. Chem. Phys.* **75**, 2800 (1981); R. S. Berry, H. L. Davis, and T. L. Beck, *Chem. Phys. Lett.* **147**, 13 (1988); D. T. Nguyen and D. A. Case, *J. Phys. Chem.* **89**, 4020 (1985); T. Lazaridis, D. J. Tobias, C. L. Brooks III, and M. E. Paulaitis, *J. Chem. Phys.* **95**, 7612 (1991).
- ²K. Müller and L. D. Brown, *Theor. Chim. Acta (Berlin)* **53**, 75 (1979).
- ³K. Müller, *Angew. Chem. Int. Ed. Engl.* **19**, 1 (1980).
- ⁴S. Fischer and M. Karplus, *Chem. Phys. Lett.* **96**, 5272 (1992); J. E. Sinclair and R. Fletcher, *J. Phys. C: Solid State Phys.* **7**, 864 (1974).
- ⁵A. Ulitsky and D. Shalloway, *J. Chem. Phys.* **106**, 10099 (1997).
- ⁶R. Elber and M. Karplus, *Chem. Phys. Lett.* **139**, 375 (1987).
- ⁷L. R. Pratt, *J. Chem. Phys.* **85**, 5045 (1986).
- ⁸R. Czerminski and R. Elber, *Int. J. Quantum Chem.* **24**, 167 (1990).
- ⁹R. Czerminski and R. Elber, *J. Chem. Phys.* **92**, 5580 (1990).
- ¹⁰A. Ulitsky and R. Elber, *J. Chem. Phys.* **92**, 1510 (1990).
- ¹¹G. Mills, H. Jönsson, and G. K. Schenter, *Surf. Sci.* **324**, 305 (1995); O. S. Smart, *Chem. Phys. Lett.* **222**, 503 (1994).
- ¹²R. Elber, in *Recent Developments in Theoretical Studies of Proteins*, edited by R. Elber (World Scientific, Singapore, 1996).
- ¹³P. G. Wolynes, in *Complex Systems, SFI Studies in the Sciences of Complexity*, edited by D. L. Stein, (Addison-Wesley Longman, 1989).
- ¹⁴L. Onsager and S. Machlup, *Phys. Rev.* **91**, 1505, 1512 (1953).
- ¹⁵R. Olender and R. Elber, *J. Chem. Phys.* **105**, 9299 (1996).
- ¹⁶R. E. Gillian and K. R. Wilson, *J. Chem. Phys.* **97**, 1757 (1992).
- ¹⁷J. E. Straub, B. J. Berne, and B. Roux, *J. Chem. Phys.* **93**, 6804 (1990); C. L. Brooks III and S. A. Adelman, *J. Chem. Phys.* **77**, 4845 (1982).
- ¹⁸D. G. Truhlar and B. C. Garrett, *Acc. Chem. Res.* **13**, 440 (1980).
- ¹⁹C. W. Gardiner, *Handbook of Stochastic Methods* (Springer, New York, 1983).
- ²⁰B. J. Berne, M. Borkovec, and J. E. Straub, *J. Phys. Chem.* **92**, 3711 (1988).
- ²¹A. M. Berezhkovskii, L. M. Berezhkovskii, and V. Yu. Zitzerman, *Chem. Phys.* **130**, 55 (1989).
- ²²R. S. Larson, *Physica A* **137**, 295 (1986).
- ²³M. Berkowitz, J. D. Morgan, J. A. McCammon, and S. H. Northrup, *J. Chem. Phys.* **79**, 5563 (1983).
- ²⁴A more general definition of the path of least resistance was presented for the case of isotropic, spatially dependent friction $\gamma(\mathbf{r})$ (Ref. 23). It was defined as the path which minimizes the line integral $\mathcal{R} = \int_{\mathbf{r}_R}^{\mathbf{r}^*} e^{\beta \mathcal{W}(\mathbf{r})} d\mathbf{l}(\mathbf{r})$. The effective potential $\mathcal{W}(\mathbf{r}) = U(\mathbf{r}) + k_B T \ln[\gamma(\mathbf{r})/\gamma(\mathbf{r}_R)]$, where $\gamma(\mathbf{r}_R)$ is the friction at an arbitrarily chosen reference point.

For the case of spatially independent friction γ considered in this work $\mathcal{W}(\mathbf{r})=U(\mathbf{r})$. In general, it is best to optimize \mathcal{R} rather than \mathcal{P} . However, while methods exist for the calculation of spatially dependent diffusion tensors (Refs. 17 and 28) the calculation of the friction along all coordinates in a multidimensional space remains computationally forbidding.

²⁵P. Amara and J. E. Straub, *J. Phys. Chem.* **99**, 14 840 (1995).

²⁶K. Fukui, S. Kato, and H. Fujimoto, *J. Am. Chem. Soc.* **97**, 1 (1975).

²⁷B. R. Brooks, R. Bruccoleri, B. Olafson, D. States, S. Swainathan, and M. Karplus, *J. Comput. Chem.* **4**, 187 (1983).

²⁸J. E. Straub, M. Borkovec, and B. J. Berne, *J. Phys. Chem.* **91**, 4995 (1987).